

Droplet collisions after liquid jet breakup in microgravity conditions

This article has been downloaded from IOPscience. Please scroll down to see the full text article.

2011 J. Phys.: Conf. Ser. 327 012026

(<http://iopscience.iop.org/1742-6596/327/1/012026>)

View [the table of contents for this issue](#), or go to the [journal homepage](#) for more

Download details:

IP Address: 147.83.119.151

The article was downloaded on 20/01/2012 at 16:49

Please note that [terms and conditions apply](#).

Droplet collisions after liquid jet breakup in microgravity conditions

Francesc Suñol and Ricard González-Cinca

Departament de Física Aplicada, Barcelona Tech-Universitat Politècnica de Catalunya
Esteve Terradas 5, 08860 Castelldefels (Barcelona), Spain

E-mail: francesc@fa.upc.edu, ricard@fa.upc.edu

Abstract. The droplet dynamics and collisions after a liquid jet breakup have been experimentally studied in low gravity conditions. An experimental setup was designed in order to be used at the I.N.T.A. Drop Tower, which allows for 2.1 seconds of microgravity. The dynamics of distilled water jets injected into a rectangular tank was recorded by means of a high-speed video camera. Observations of the droplet trajectories showed a conical shape of the liquid jet caused by droplet collisions just after detachment from the liquid jet. The detached droplets initially follow straight paths at constant velocity in the direction of injection. Deviation of these trajectories is a consequence of the collision between two droplets with an impact parameter slightly different from zero. The collision between two droplets can give rise to coalescence or bouncing between droplets depending on the droplet velocity difference and impact parameter. At low values of the relative velocity, the collision leads to coalescence between droplets, while at higher values the collision results in bouncing between droplets.

1. Introduction

Liquid jets are encountered in a very large variety of natural and technological environments. The structure of liquid jets has been widely studied in the last century, due to its fundamental importance and practical applications in different fields. Nevertheless, the improvement of computer processing power, high-speed photography, and other laboratory techniques has recently attracted increasing attention to the subject.

On the analytical side, studies on liquid jets started with the work of Lord Rayleigh [1] and have been conducted in order to describe the breakup mechanisms. The fundamental tool is the linear stability analysis around the cylindrical base state, although later research refined this analysis to include the effects of viscosity, outside fluid effects, nozzle geometry, etc. [2–4]. In addition, many non-linear effects are dominant in the breakup process. Although these effects are extremely difficult to implement numerically, promising advances have been recently carried out [5–8].

From an experimental point of view, advances in numerous techniques have made possible the detailed study of the breakup process [9–13] and the structure of the resulting fragments [14–16]. In particular, the bouncing and coalescence of the resulting droplets [17–19]. Hence, a considerable amount of information can be provided for comparison with theory. However, experimental results have generally been obtained in normal gravity, with the jet injection direction aligned with the gravity force. The gravity force can be predominant in the dynamics of such flows, and it can mask the effects of inertia and surface tension. For this reason, a

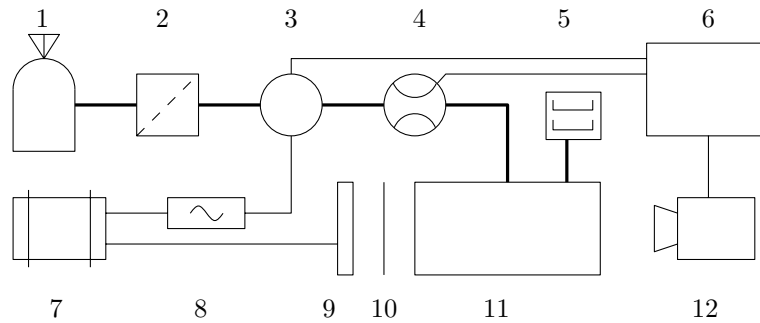


Figure 1. Sketch of the experimental setup. Thin lines: Electric connections. Thick lines: Hydraulic connections. 1: Liquid reservoir. 2: Filter. 3: Liquid pump. 4: Liquid flow meter. 5: Residual tank. 6: PC. 7: Batteries (power supply). 8: DC/AC inverter. 9: LED matrix. 10: Diffuser sheet. 11: Test tank. 12: High-speed camera.

microgravity environment is required to investigate the effects of the inertial and surface forces without the masking effects of gravity.

Umemura et al. [12] and Tsukiji et al. [13] studied the atomization regimes of a liquid jet in microgravity. The jet emerged into a gas whose temperature and pressure exceeded the critical values of the injected liquid, identifying a new hydrodynamic-assisted capillary instability. The parameter range in their investigations differs notably from the one used in the present work.

In this study, we focus on the structure of a jet after breakup by the Rayleigh mode in a low gravity environment. The breakup mechanism is determined by a direct competition between the surface and the inertial forces. The surface tension between fluids amplifies the jet surface perturbations until the radius of the perturbations equals the radius of the initial jet. At this instant, a droplet is created. This breakup mechanism occurs at low velocities and leads to the formation of droplets with a larger diameter than the initial jet diameter. On ground, the generated droplets follow a rectilinear path in a two-dimensional space initially in the direction of injection, with an increasing velocity due to gravity. The dynamics of droplets in microgravity is different. The collision between droplets after detachment gives rise to a resulting jet of conical shape, whilst the droplets follow rectilinear paths between collisions in a three-dimensional space.

A description of the experimental setup is provided in Section 2. The obtained results and discussion is presented in Section 3. Conclusions are finally drawn in Section 4.

2. Experimental setup

With the aim of studying the droplet dynamics and collisions after liquid jet breakup in a microgravity environment, an experimental setup was designed in order to be used at the I.N.T.A. Drop Tower (Torrejón de Ardoz, Spain), which allows for 2.1 seconds at 10^{-4} - 10^{-5} g.

Liquid jets were injected into a stainless steel rectangular tank (with a length of 160 mm, width of 200 mm and height of 250 mm) provided with two methacrylate windows which allow the visualization of the interior of the tank. The working liquid was distilled water, with a density of $\rho = 998 \text{ kg/m}^3$, viscosity $\mu = 1 \cdot 10^{-3} \text{ Pa}\cdot\text{s}$, and surface tension $\sigma = 7.28 \cdot 10^{-2} \text{ N/m}$. Water was directed to the test tank from a pump (Ismatec MCP-Z Standard) connected to a nozzle, and the liquid flow rate Q_L was measured using a Bronkhorst L30 liquid flow meter. Liquid flow rates were increased from 5 ml/min up to 15 ml/min. The nozzle internal and external diameter were $d = 0.7 \text{ mm}$ and $D = 1.8 \text{ mm}$, respectively. The experiments were conducted at room temperature (around 20° C) and at ambient pressure. A RedLake MotionXtra HG-SE high-speed camera recorded the jets at framerates between 500 and 1000 frames per second

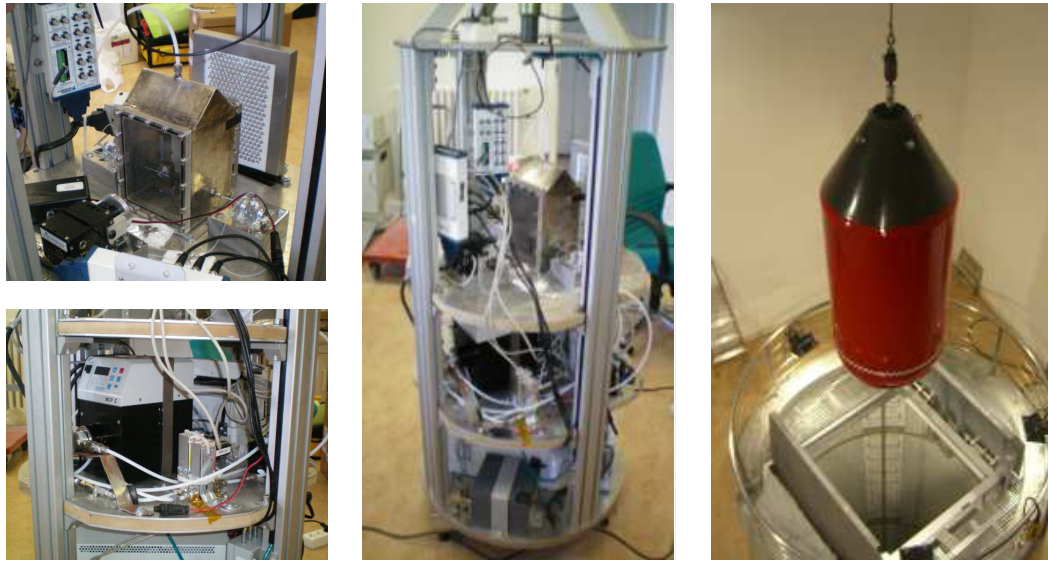


Figure 2. Pictures of the experimental rack (left and middle) and the capsule containing it (right) at the I.N.T.A. drop tower. Left: detail of the first and second floors of the rack; middle: whole rack.

(recording images at 640×512 and 640×256 pixels, respectively), depending on the experiment run. The high-speed camera had a built-in battery and an internal memory, and was activated by means of a trigger signal. The resolution of the acquired images was 0.15 mm per pixel. The illumination system consisted of a matrix of 280 ultrabright LEDs whose light was homogenized by a diffuser sheet. The liquid pump and the data acquisition system were controlled remotely using LabView software. A sketch of the experimental setup is presented in Fig. 1.

In Fig. 2, some pictures of the experimental setup in the capsule rack are shown. Equipment was distributed in three floors. Batteries were placed in the first floor. Test tank, illumination system and high-speed camera were placed in the second floor. In the third floor, there were the liquid pump, liquid flow meter, DC/AC inverter, liquid reservoir and residual tank.

3. Results and discussion

3.1. Droplet trajectories

In order to measure the droplet trajectories, an automatized method for tracking from the recorded videos the droplet centers evolving in time has been used.

In Fig 3, an x - y map (being x the injection direction) of the droplet trajectories for the case of $Q_L = 15$ ml/min is presented. It can be observed that the trajectories with the highest slope do not cross the origin (being the origin the average breakup point). In the video analysis one observes that the droplets created after the jet breakup maintain a horizontal trajectory following the direction of injection. The deflected trajectories are a consequence of droplet collisions, most of them taking place near the jet breakup point. Droplet collisions occur when a drop moving in the injection direction is followed by a slightly faster drop moving in the same direction with a low impact parameter different from zero. After the collision, the trajectories of the droplets are deviated from the injection direction. The collision process is shown in Figure 4: two droplets with impact parameter $b \neq 0$ are approaching each other with $|\vec{v}_1| < |\vec{v}_2|$. Although the initial velocities are in the injection direction (time t_1 in Fig. 4), after the collision both velocities have a non-zero component perpendicular to the direction of injection (time t_3 in Fig. 4).

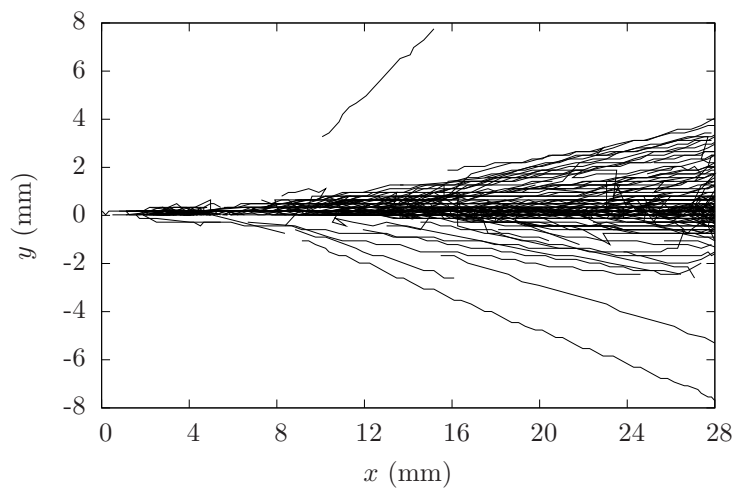


Figure 3. Map of droplet trajectories for $Q_L = 15$ ml/min.

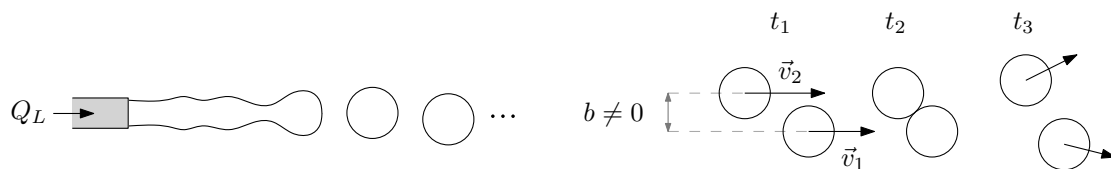


Figure 4. Collision process.

The deviation of the droplet trajectory can also be the result of multiple collisions or bounces. In Figure 5(a), a double bouncing is illustrated. At $t = 0$, a droplet is generated with a velocity v_1 in the injection direction. The following generated droplet (with a slightly smaller diameter) has a higher velocity v_2 in the direction of injection ($|v_2| > |v_1|$), and collides with the first droplet at $t = 8$ ms. At this point, v_2 is abruptly reduced, and a third droplet with velocity v_3 in the injection direction ($|v_3| > |v_2|$) collides with the second droplet at $t = 20$ ms. Since the second and third droplets have an impact parameter b different from zero, their trajectories are deviated with respect to the injection direction. This phenomenon can only be observed in microgravity conditions, since in normal gravity the acceleration of the droplets after detachment prevents the droplets from collisions.

In Figure 5(b), the time evolution of two colliding droplets is presented. In this case the collision gives rise to a coalescence phenomenon at $t = 3$ ms. Thus, in the range of droplet sizes and velocities of this work, the impact between two droplets can result in either bouncing or coalescence.

3.2. Droplet collisions: bouncing and coalescence

After a collision, droplets can bounce or coalesce. Considering that inertia and surface tension are key factors in these phenomena, the Weber number turns out to be an appropriate parameter of study. Taking into account the relative velocity $v_{rel} = v_i - v_j$ between droplets i and j prior to collision, a modified Weber number We^* is introduced,

$$We^* = \frac{\rho v_{rel}^2 d^*}{\sigma}, \quad (1)$$



Figure 5. Time evolution of (a) Double bouncing process, (b) Coalescence process.

where $d^* = \sqrt{d_i d_j}$, being d_i and d_j the equivalent diameter of droplet i and j , respectively.

In Fig. 6, a map of the observed phenomena for given normalized impact parameter and modified Weber number is presented. Only four values of b/d (which correspond to 0, 1, 2 and 3 pixels) could be considered, due to the actual spatial resolution of the images.

Despite the few data points available, one can observe a tendency of coalescence taking place at low modified Weber numbers, while bouncing occurs more frequently at high values of We^* . This may seem to be in contrast with the results obtained by Gao et al. [14] and Ko and Ryou [15] using ethanol and water droplet collisions, or the results from Chen and Chen [16] using diesel oil and water droplet collisions. In their works, bouncing is observed at lower We^* and coalescence at higher values. However, the values of We^* in their studies were larger than in the present work. Furthermore, in investigations of Orme, Willis and Passandideh and coworkers [17–19] an additional regime of coalescence at low values of the modified Weber number was found.

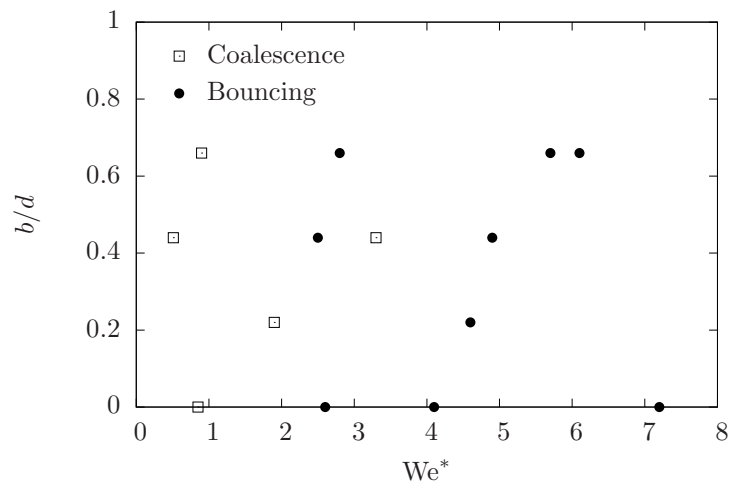


Figure 6. Observed phenomena (coalescence or bouncing) for given normalized impact parameter b/d and modified Weber number.

4. Conclusions

An experimental setup for the study of droplet dynamics and collisions in microgravity has been presented. Several experiments were run with this setup at the I.N.T.A Drop Tower. The most remarkable results obtained from the experiments can be summarized in the following points:

- A conical-shaped jet is observed in the region where droplets detach and move away from the initial jet. The conical shape is neither due to the rectilinear trajectories of the droplets detaching from the nozzle nor to the breakup phenomenon. The shape of the droplet jet is obtained from the bouncing process between colliding droplets just after detachment. This conclusion has been obtained from the trajectories of individual droplets, observing that the vertex of the cone has a positive offset in the injection direction, with respect to the jet breakup point.
- Droplet collisions at low values of the relative velocity result in coalescence. On the contrary, at higher values of the relative velocity, collisions result in bouncing between droplets.

Acknowledgments

We are thankful to I.N.T.A for their assistance and support in the payload integration. We acknowledge *Ministerio de Ciencia e Innovación* (Spain) for financial support (Project number AYA-2009-11493). F. S. also acknowledges *Comissionat per a Universitats i Recerca del Departament d'Innovació, Universitats i Empresa de la Generalitat de Catalunya i del Fons Social Europeu*.

References

- [1] Rayleigh L 1878 On the instability of jets *Proc. of the London Math. Soc.* **10** 4.
- [2] Teng H, Kinoshita C M, and Masutani S M 1995 *Int. J. Multiphase Flow* **21** 129.
- [3] Lin S P and Reitz R D 1998 *Annu. Rev. Fluid Mech.* **30** 85.
- [4] Eggers J and Villiermaux E 2008 *Rep. Prog. Phys.* **71** 036601.
- [5] Ménard T, Tanguy S and Berlemont A 2002 *Int. J. Multiphase Flow* **33** (5) 510.
- [6] Fuster D, Bagué A, Boeck T, Le Moyne L, Leboissetier A, Popinet S, Ray P, Scardovelli R and Zaleski S 2009 *Int. J. Multiphase Flow* **35** (6) 550.
- [7] Lebas R, Ménard T, Beau P A, Berlemont A and Demoulin F X 2009 *Int. J. Multiphase Flow* **35** (3) 247.
- [8] Delteil J, Vincent S, Erriguible A and Subra-Paternault P 2011 *Computers and Fluids* Accepted manuscript - doi:10.1016/j.compfluid.2011.05.010.

- [9] Reitz R D and Bracco F V 1982 *Phys. Fluids* **25** 1730.
- [10] Liu Z and Reitz R D 1997 *Int. J. Multiphase Flow* **23** (4) 631.
- [11] Lasheras J C and Hopfinger E J 2000 *Ann. Rev. of Fluid Mech.* **32** 275.
- [12] Umemura A and Wakashima Y 2002 *Proc. of the Comb. Inst.* **29** 633.
- [13] Tsukiji H, Umemura A and Hisida M 2004 *Proc. of the Conf. on Aerospace Prop* 97.
- [14] Gao T C, Chen R H and Lin T H 2005 *Experiments in Fluids* **38** 731.
- [15] Ko G H and Ryou H S 2005 *Int. Journal of Multiphase Flow* **31** 723.
- [16] Chen R H and Chen C T 2006 *Experiments in Fluids* **41** 453.
- [17] Orme M 1997 *Prog. Energy Combust. Sci.* **23** 65.
- [18] Willis K and Orme M 2003 *Experiments in Fluids* **34** 28.
- [19] Passandideh-Fard M and Roohi E 2006 *14th Annual (International) Mechanical Engineering Conference* Isfahan University of Technology (Iran).